INT. J. NUM. METH. HEAT FLUID FLOW, VOL. 5, 589–600 (1995)

A SIMULTANEOUS ITERATION PROCEDURE FOR THE FINITE ELEMENT SOLUTION OF THE ENTHALPY MODEL FOR PHASE CHANGE HEAT CONDUCTION PROBLEMS

ZHEN-XIANG GONG AND ARUN S. MUJUMDAR

Department of Chemical Engineering, McGill University, Montreal, Quebec, Canada H3A 2A7

ABSTRACT

Based on a lumped mass model and an incremental iteration method, an efficient simultaneous iteration procedure is developed for the finite element solution of the enthalpy model. This procedure uses Gauss elimination to solve the resulting algebraic equation system. A one-point quadrature program based on the isoparametric quadrilateral element is incorporated for the calculation of the heat conductance matrix, leading to a significant reduction of the computation time.

KEY WORDS Finite element Enthalpy One point quadrature

INTRODUCTION

The enthalpy model proposed by Shamsundar and Sparrow[1] is one of the most popular approaches to the solution of phase change heat conduction problems. In this model, both enthalpy and temperature are included in the field equation as dependent variables; therefore, n equations emerge containing $2n$ dependent variables in the final discrete algebraic equations. Gauss–Siedel iteration, or an equivalent non-simultaneous iteration procedure, is required to solve the algebraic equations along with the equations of state. As such schemes provide slow convergence, especially due to the phase change non-linearity, a large number of iterations are required in each time step, particularly for two and three dimensional problems.

Enthalpy concepts have been applied for phase change problems since 1974 (please see the pioneering paper by Comini *et al.*[2] and the improved version of their method[3,4,12]) but not in the way Shamsundar and Sparrow have proposed. The procedures developed in references 2–4, 12 have been well established and are effective in solving phase change problems. However, these procedures are, in fact, different combinations of the enthalpy concept with the equivalent heat capacity method.

The enthalpy model of Shamsundar and Sparrow has always been associated with finite difference rather than finite element methods. It is partly due to, in the authors' opinion, the feature of the enthalpy model which makes the solution procedure of the finite element method both inefficient and a little difficult to implement since most of the existing finite element programs are equipped with direct solvers.

0961–5539/95/070589–12$2.00

Received October 1993
Revised May 1994

In this paper the finite element method is used to solve the enthalpy model. A new efficient simultaneous iteration procedure is developed to solve the final discrete matrix equation. This procedure uses Gauss elimination to solve the algebraic equations and is easy to implement with any existing finite element heat conduction computer program with only a little modification. The isoparametric bilinear quadrilateral element is employed and a one-point quadrature algorithm[5,6] is incorporated into the calculation of the thermal conductance matrices, reducing greatly the computation time.

MATHEMATICAL FORMULATION

The mathematical description of the enthalpy model for phase change heat conduction problems, following Shamsundar and Sparrow[1], is as follows:

$$\frac{\partial(\rho H)}{\partial t} - \nabla\cdot(k\nabla T) = 0, \qquad x\in\Omega\subset R^3,\ t\in[0,t] \tag{1}$$

in which ρ is density, H enthalpy per unit mass, t time, k thermal conductivity, T temperature, x space coordinate, Ω solution domain, R^3 three-dimensional space, and:

$$(\rho,k) = \begin{cases}\rho,k_s & H < H_s^* \\ \rho,k_l & H > H_l^*\end{cases} \tag{2}$$

in which (and in subsequent equations) subscripts s and l represent solid and liquid phases, respectively; superscript * denotes the state of saturation

Equation (1) is coupled with the following equations of state:

$$T - T_m = \begin{cases}(H - H_s^*)/c_s & H < H_s^* \\ 0 & H_s^* \leqslant H \leqslant H_l^* \\ (H - H_l^*)/c_l & H_l^* < H\end{cases} \tag{3}$$

where T_m is the discrete melting temperature and c is the specific heat.

FINITE ELEMENT DISCRETIZATION

The spacewise discretization of (1) can be accomplished using the standard Galerkin's method[7]. Multiplying (1) by a weight function W_I and integrating it over the solution domain Ω, we have:

$$\int_\Omega W_I \frac{\partial(\rho H)}{\partial t}\,\mathrm{d}\Omega - \int_\Omega W_I[\nabla\cdot(k\nabla T)]\,\mathrm{d}\Omega = 0 \tag{4}$$

Integration by parts results in:

$$\int_\Omega W_I \frac{\partial(\rho H)}{\partial t}\,\partial\Omega + \int_\Omega \nabla W_I\cdot(k\nabla T)\,\mathrm{d}\Omega - \int_\Omega \nabla\cdot[W_I(k\nabla T)]\,\mathrm{d}\Omega = 0 \tag{5}$$

After making use of Green's theorem, in order to obtain the boundary integral of the domain, we have:

$$\int_\Omega W_I \frac{\partial(\rho H)}{\partial t}\,\mathrm{d}\Omega + \int_\Omega \nabla W_I\cdot(k\nabla T)\,\mathrm{d}\Omega - \oint_\Gamma W_I[(k\nabla T)\cdot\mathbf{n}]\,\mathrm{d}\Gamma = 0 \tag{6}$$

in which Γ is the boundary of the solution domain and $\mathbf{n}$ is the outward normal of the boundary. The boundary integral vanishes in the case of the Dirichlet boundary condition and for zero

heat flux, $k\nabla T \cdot \mathbf{n} = 0$, at the boundaries. For the Robin boundary condition (boundary condition of the third kind), the boundary integral is:

$$-\oint_\Gamma W_I[(k\nabla T)\cdot\mathbf{n}]\,d\Gamma = \oint_\Gamma W_I h(T - T_f) \tag{7}$$

in which h is the convection heat transfer coefficient and T_f is the ambient temperature.

Let the unknown functions H and T be approximated throughout the solution domain at any time t by:

$$H = \sum_{I=1}^{m} N_I(x, y, z)H_I(t) \tag{8}$$

and

$$T = \sum_{I=1}^{m} N_I(x, y, z)T_I(t) \tag{9}$$

where N_I ($I = 1, 2, \ldots, m$; m is the nodal number of each element) are the usual shape functions defined piecewise element by element; H_I and T_I the nodal parameters. Substituting (8) and (9) into (6) and then replacing the weight function W_I by the shape function N_I, we obtain the following matrix differential equation:

$$[M(T)]\{\dot{H}\} + [K(T)]\{T\} = \{F(T)\} \tag{10}$$

in which $[M(T)]$ is the heat capacity matrix, $[K(T)]$ the conductance matrix and $\{F(T)\}$ the heat load vector. The superposed dot '$\cdot$' denotes differentiation with respect to time. Typical matrix elements are:

$$M_{IJ} = \sum \int_{\Omega^e} \rho N_I N_J \,d\Omega \tag{11}$$

$$K_{IJ} = \sum \int_{\Omega^e} \nabla N_I k \nabla N_J \,d\Omega + \sum \int_{\Gamma^e} h N_I N_J \,d\Gamma \tag{12}$$

$$F_I = \sum \int_{\Gamma^e} h N_I T_f \,d\Gamma \tag{13}$$

In the above equations, standard indicial notation is used with repeated subscripts implying summation; Ω^e is the element region and Γ^e refers only to elements with external boundaries on which the third kind boundary condition is specified.

TIME DISCRETIZATION

Discretization of the time derivative in (10) is most often achieved with a finite difference technique. Although many time-stepping schemes are available[8,9], the most popular ones are the two-time-level methods. In this work, a predictor-corrector scheme[10,11] is used.

Predictor:
$$\{\tilde{H}_{n+1}\} = \{H_n\} + (1 - \alpha)\Delta t\{\dot{H}_n\} \tag{14}$$

Corrector:
$$\{H_{n+1}^{i+1}\} = \{\tilde{H}_{n+1}\} + \alpha\Delta t\{\dot{H}_{n+1}^{i+1}\} \tag{15}$$

Correspondingly,

$$\{\tilde{T}_{n+1}\} = \{T_n\} + (1 - \alpha)\Delta t\{\dot{T}_n\} \tag{16}$$

$$\{T_{n+1}^{i+1}\} = \{\tilde{T}_{n+1}\} + \alpha\Delta t\{\dot{T}_{n+1}^{i+1}\} \tag{17}$$

In the preceding equations, subscript n denotes the nth time step, superscript i designates the ith iteration, α is an integral parameter which controls the accuracy and the stability of the time integration, $\alpha = 0 \sim 1$ and Δt is the time step of time integration.

Substitution of (17) into (10) leads to:

$$[M(T^i_{n+1})]\{\dot{H}^{i+1}_{n+1}\} + \alpha\Delta t[K(T^i_{n+1})]\{\dot{T}^{i+1}_{n+1}\} = \{F(T^i_{n+1})\} - [K(T^i_{n+1})]\{\tilde{T}_{n+1}\} \tag{18}$$

Since the following relationship exists between the enthalpy and temperature for heat conduction without phase change:

$$\mathrm{d}H = c\,\mathrm{d}T \tag{19}$$

we can obtain:

$$\{\dot{H}\} = [C]\{\dot{T}\} \tag{20}$$

if the lumped mass model[7,12] is adopted. Here $[C]$ is the heat capacity matrix and is diagonal. Equation (20) can easily be transformed into:

$$\{\dot{T}\} = [C]^{-1}\{\dot{H}\} \tag{21}$$

since $[C]$ is a diagonal matrix.

Equation (21) is not valid if a phase change takes place in the heat conduction processed. This is due to the fact that the temperature rates of those nodes in which a phase change is taking place are equal to zero but the enthalpy rates are not. However, it can still hold true if the conductance matrix on the left hand side of (18), which will consist of the global matrix of the final discrete equation system, is modified such that all the elements in column I are set equal to zero if phase change is taking place in node I.

As a further explanation, take an element (bilinear quadrilateral element used in this study), for example, if there is no phase change at all nodes of the element, the following equation is valid:

$$[K_{IJ}]_e\{\dot{T}_J\}_e = [K_{IJ}]_e\{\dot{H}_J/C_{JJ}\}_e = [K_{IJ}]_e[C_{IJ}]_e^{-1}\{\dot{H}_J\}_e \tag{22}$$

in which subscript e denotes the element and subscripts $I, J = 1, 2, 3, 4$; while if phase change is taking place, for example, at node 1, there is $\dot{T}_1 = 0$, and then,

$$\begin{aligned}
[K_{IJ}]_e\{\dot{T}_J\}_e &= \begin{bmatrix} K_{11} & K_{12} & K_{13} & K_{14} \\ K_{21} & K_{22} & K_{23} & K_{24} \\ K_{31} & K_{32} & K_{33} & K_{34} \\ K_{41} & K_{42} & K_{43} & K_{44} \end{bmatrix} \begin{Bmatrix} 0 \\ \dot{T}_2 \\ \dot{T}_3 \\ \dot{T}_4 \end{Bmatrix} = \begin{bmatrix} 0 & K_{12} & K_{13} & K_{14} \\ 0 & K_{22} & K_{23} & K_{24} \\ 0 & K_{32} & K_{33} & K_{34} \\ 0 & K_{42} & K_{43} & K_{44} \end{bmatrix} \begin{Bmatrix} \dot{T}_1 \\ \dot{T}_2 \\ \dot{T}_3 \\ \dot{T}_4 \end{Bmatrix} \\
&= \begin{bmatrix} 0 & K_{12} & K_{13} & K_{14} \\ 0 & K_{22} & K_{23} & K_{24} \\ 0 & K_{32} & K_{33} & K_{34} \\ 0 & K_{42} & K_{43} & K_{44} \end{bmatrix} \begin{Bmatrix} \dot{H}_1/C_{11} \\ \dot{H}_2/C_{22} \\ \dot{H}_3/C_{33} \\ \dot{H}_4/C_{44} \end{Bmatrix} \\
&= \begin{bmatrix} 0 & K_{12} & K_{13} & K_{14} \\ 0 & K_{22} & K_{23} & K_{24} \\ 0 & K_{32} & K_{33} & K_{34} \\ 0 & K_{42} & K_{43} & K_{44} \end{bmatrix} \begin{bmatrix} 1/C_{11} & & & \\ & 1/C_{22} & & \\ & & 1/C_{33} & \\ & & & 1/C_{44} \end{bmatrix} \begin{Bmatrix} \dot{H}_1 \\ \dot{H}_2 \\ \dot{H}_3 \\ \dot{H}_4 \end{Bmatrix} \\
&= [K^{\#}_{IJ}]_e[C_{IJ}]_e^{-1}\{\dot{H}_J\}_e
\end{aligned} \tag{23}$$

in which $[K^{\#}_{IJ}]_e$ is the modified element conductance matrix.

Substitution of (21) into (18) yields:

$$\{[M(T^i_{n+1})] + \alpha\Delta t[K^{\#}(T^i_{n+1})][C(T^i_{n+1})]^{-1}\}\{\dot{H}^{i+1}_{n+1}\} = \{F(T^i_{n+1})\} - [K(T^i_{n+1})]\{\bar{T}_{n+1}\} \quad (24)$$

where $[K^{\#}(T^i_{n+1})]$ is the modified conductance matrix.

Since (24) is highly nonlinear, an incremental iteration technique[7] is employed to effect a solution. As a result, (24) becomes:

$$[K^{@}(T^i_{n+1})]\{\Delta\dot{H}\} = \{R(T^i_{n+1})\} \quad (25)$$

where,

$$\{R(T^i_{n+1})\} = \{F(T^i_{n+1})\} - [K(T^i_{n+1})]\{T^i_{n+1}\} - [M(T^i_{n+1})]\{\dot{H}^i_{n+1}\} \quad (26)$$

$$[K^{@}(T^i_{n+1})] = [M(T^i_{n+1})] + \alpha\Delta t[K^{\#}(T^i_{n+1})][C(T^i_{n+1})]^{-1} \quad (27)$$

and $\{\Delta\dot{H}\}$ is the increment of $\{\dot{H}\}$ in each iteration.

Originally, the conductance matrix $[K]$ is symmetrical. A modification, such as that mentioned above, as well as the multiplication of $[K^{\#}][C]^{-1}$ makes $[K^{@}]$ asymmetrical. This is illustrated at the element level by the following equation:

$$[K^{\#}_{IJ}]_e[C_{IJ}]_e^{-1} = \begin{bmatrix} 0 & K_{12}/C_{22} & K_{13}/C_{33} & K_{14}/C_{44} \\ 0 & K_{22}/C_{22} & K_{23}/C_{33} & K_{24}/C_{44} \\ 0 & K_{23}/C_{22} & K_{33}/C_{33} & K_{34}/C_{44} \\ 0 & K_{24}/C_{22} & K_{34}/C_{33} & K_{44}/C_{44} \end{bmatrix} \quad (28)$$

The asymmetrical matrix is a drawback of the procedure. However, $[K^{@}]$ can be made symmetric if the modified conductance matrix is further modified such that all the elements in row i in $[K^{\#}_{IJ}]$ are also taken to be zero if a phase change is taking place at node I, and the two sides of (25) are multiplied by the same matrix $[C]^{-1}$. The symmetrization process is illustrated at the element level by the following equation:

$$[C_{IJ}]_e^{-1}[K^{\#\#}_{IJ}]_e[C_{IJ}]_e^{-1} = \begin{bmatrix} 0 & 0 & 0 & 0 \\ 0 & K_{22}/C^2_{22} & K_{23}/C_{22}C_{33} & K_{24}/C_{22}C_{44} \\ 0 & K_{23}/C_{33}C_{22} & K_{33}/C^2_{33} & K_{34}/C_{33}C_{44} \\ 0 & K_{24}/C_{44}C_{22} & K_{34}/C_{44}C_{33} & K_{44}/C^2_{44} \end{bmatrix} \quad (29)$$

where $[K^{\#\#}_{IJ}]_e$ is the further modified element conductance matrix. This further modification does not affect the final results as when the iteration converges in (25), $\{\Delta\dot{H}\} = \{0\}$, with the result $\sum K^{@}_{IJ}\Delta\dot{H}_J = 0$. This is attributed to the selection of the increment of enthalpy rate as the variable to be solved.

As will be seen in the subsequent numerical examples, the symmetrization of the global matrix in the final discrete matrix equation, (25), may increase the iteration number in each time step, but can lead to reductions in the memory requirement and in the computational effort in equation solving, with the consequence of a probable reduction in the total computation time, especially for problems requiring a great number of nodes. Since $[C]$ is diagonal, calculation of $[C]^{-1}$ and the multiplication of $[C]^{-1}$ require only a small computational effort.

After further modification of the conductance matrix and multiplication of $[C]^{-1}$ at the two sides of (25), we have:

$$[K^{\&}(T^i_{n+1})]\{\Delta\dot{H}\} = \{R^{\&}(T^i_{n+1})\} \quad (30)$$

where

$$\{R^{\&}(T^i_{n+1})\} = [C]^{-1}\{R(T^i_{n+1})\} \quad (31)$$

$$[K^{\&}(T^i_{n+1})] = [C]^{-1}[K^{@}(T^i_{n+1})] \quad (32)$$

Gauss elimination is used to solve (30). The solution steps are as follows:

(1) With the initial temperature distribution, calculate the initial enthalpy field with (3).
(2) At the beginning of each time step, for $i = 0$, calculate $\{\tilde{H}_{n+1}\}$ according to (14), and then set $\{H^0_{n+1}\} = \{\tilde{H}_{n+1}\}$; $\{\dot{H}^0_{n+1}\} = \{0\}$.
(3) With the two starting vectors, $\{\Delta\dot{H}\}$ is obtained by solving (30).
(4) Update $\{\dot{H}^{i+1}_{n+1}\}$ by $\{\dot{H}^{i+1}_{n+1}\} = \{\dot{H}^{i}_{n+1}\} + \{\Delta\dot{H}\}$ and $\{H^{i+1}_{n+1}\}$ using (15).
(4) If the convergence condition is met (here, we compare the Euclidean norms of $\{\Delta\dot{H}\}$ and $\{R\}$ to some selected constants TOL1 and TOL2), set $\{H_{n+1}\} \overset{\text{df}}{=} \{H^{i+1}_{n+1}\}$ and $\{\dot{H}_{n+1}\} \overset{\text{df}}{=} \{\dot{H}^{i+1}_{n+1}\}$; if not, with $\{\dot{H}^{i+1}_{n+1}\}$ and $\{H^{i+1}_{n+1}\}$ as starting vectors, go to step (3) to undertake the next iteration.

It should be noted that extension of the procedure described above to other time-stepping scheme (e.g. three-time-level scheme) is direct.

ONE-POINT QUADRATURE

Because of the continuous changes of the thermal conductivity during the phase change process, the element conductance matrices have to be calculated at each iteration in every time step. This calculation occupies a large portion of the total computational work. For the isoparametric bilinear quadrilateral element used in this study, the calculation of the element conductance matrices is performed by numerical quadrature and a 2×2 Gauss quadrature is required. This is very time-consuming. In order to speed up the computation, a one-point quadrature algorithm[5,6] is incorporated into the procedure.

The shape functions for a bilinear quadrilateral element are written in a reference plane ξ, η in the form

$$N_I = \tfrac{1}{4}(1 + \xi_I\xi)(1 + \eta_I\eta) \tag{33}$$

where ξ_I, η_I are the ξ, η coordinates of node I. If one-point quadrature is used, the integrals in (11)–(13) can be computed by simply evaluating the integrands at $\xi = 0$, $\eta = 0$.

Utilization of one-point quadrature in the calculation of the conductance matrix may result in an element matrix which contains a spurious singular mode. For certain boundary conditions, this mode leads to singularity of the assembled global matrix. This drawback can be circumvented by adding a stabilization matrix to the element conductance matrix from one-point quadrature.

The heat conductance matrix by the stabilized one-point quadrature algorithm is as follows (for detailed information, refer to Reference 5):

$$[K]_e = [K]^{(1)}_e + [K]^{\text{stab}}_e \tag{34}$$

where $[K]^{(1)}_e$ is the element matrix by one-point quadrature:

$$[\mathrm{K}]^{(1)}_e = A[B]^{\mathrm{T}}[D][B] \tag{35}$$

where

$$[B] = \begin{bmatrix} N_{I,x}(0,0) \\ N_{I,y}(0,0) \end{bmatrix} = \begin{bmatrix} \{b_1\}^{\mathrm{T}} \\ \{b_2\}^{\mathrm{T}} \end{bmatrix} \tag{36}$$

Here ,x and ,y designate differentiation with respect to coordinates x and y, respectively. Further:

$$[D] = \begin{bmatrix} k & 0 \\ 0 & k \end{bmatrix} \tag{37}$$

$$\{b_1\}^T = \frac{1}{2A}[y_{24}, y_{31}, y_{42}, y_{13}] \tag{38}$$

$$\{b_2\}^T = \frac{1}{2A}[x_{42}, x_{13}, x_{24}, x_{31}] \tag{39}$$

$$x_{IJ} = x_I - x_J, \qquad y_{IJ} = y_I - y_J \tag{40}$$

and

$$A = \tfrac{1}{2}(x_{31}y_{24} + x_{24}y_{31}) \tag{41}$$

The stabilization matrix, $[K]_e^{stab}$, is given by:

$$[K]_e^{stab} = \bar{\varepsilon}A\{\gamma\}\{\gamma\}^T \tag{42}$$

where

$$\{\gamma\} = \frac{1}{A}[\{h\} - (\{h\}^T\{x\})\{b_1\} - (\{h\}^T\{y\})\{b_2\} \tag{43}$$

$$\{h\}^T = [1, -1, 1, -1] \tag{44}$$

$$\{x\}^T = [x_1, x_2, x_3, x_4] \tag{45}$$

$$\{y\}^T = [y_1, y_2, y_3, y_4] \tag{46}$$

$$\bar{\varepsilon} = \varepsilon\frac{A^2}{12}k(\{b_1\}^T\{b_1\} + \{b_2\}^T\{b_2\}) \tag{47}$$

where ε is a parameter which controls the accuracy of the integration. The fully integrated conductivity is given by $\varepsilon = 1$.

As will be demonstrated in the following section, the utilization of this stabilized one-point quadrature results in a significant reduction of computing time.

EXAMPLE CALCULATIONS

Accuracy tests

To test the accuracy of the aforementioned procedure, two illustrative problems were computed.

Solidification in a half-space

A liquid at a uniform temperature 10°C which is above its freezing point (0°C) is confined to a half-space $x > 0$. At time $t = 0$ the boundary surface at $x = 0$, is lowered to a temperature of -20°C and maintained at this temperature for $t > 0$. The thermophysical properties are as follows:

$k_s = 2.22$ W/m·K, $k_l = 0.556$ W/m·K, $c_s = 1762$ J/kg·K,
$c_l = 4226$ J/kg·K, $\rho = 1000$ kg/m^3, $\lambda = 338000$ J/kg

where λ represents the latent heat.

Two-dimensional elements are used to solve this problem although it is physically one-dimensional. The finite element mesh is shown in *Figure 1*. The length of the computed space, BC, is taken to be 1 m. Computations were carried out using 20 elements with a time

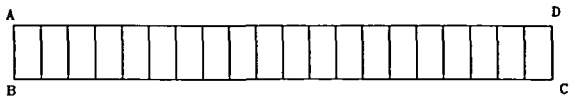

Figure 1 Finite element mesh

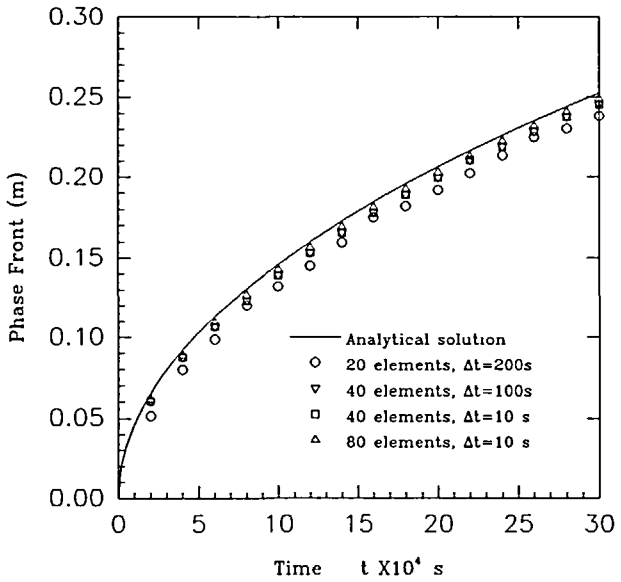

Figure 2 Comparison of the computed interface position with analytical solution

step of 200 seconds, 40 elements with a time step of 100 seconds, 40 elements with a time step of 10 seconds, as well as 80 elements with a time step of 10 seconds, respectively.

In all the computations for this problem and the following test problems, the integration parameter, α, is taken to be 0.5 and the convergence criteria TOL1 and TOL2 are taken to be 0.1 and 0.01 respectively.

Figure 2 displays a comparison of the progress of the freezing front between the computed results and the analytical solution[13]. As the slab involved is finite, comparison with the solution of a theoretical infinite slab must be terminated when the temperature begins to change appreciably at boundary DC. It can be seen from this figure that the computed results approach the exact solution with the refinement of space and time steps and the result using 80 elements with a time step of 10 seconds is in good agreement with the analytical solution.

Freezing of a corner region

The liquid in an internal corner region is initially at a uniform temperature with the surface of the wedge maintained at a uniform temperature, -1.0°C, lower than the fusion temperature (0°C). The relevent thermal properties are $k_s = k_l = 1$ W/m·K, $c_s = c_l = 1.0$ J/kg·K, $\rho = 1$ kg/m^3. In one case the initial temperature is $T_i = 0$°C and the latent heat $\lambda = 1.5613$ J/kg; in the other $T_i = 0.3$°C and $\lambda = 0.25$ J/kg.

The finite element mesh is shown in *Figure 3*. *Figure 4* shows the comparison of the present finite element results with the analytical solution[14] of the freezing front history. There is very good agreement between the computed results and the analytical solutions.

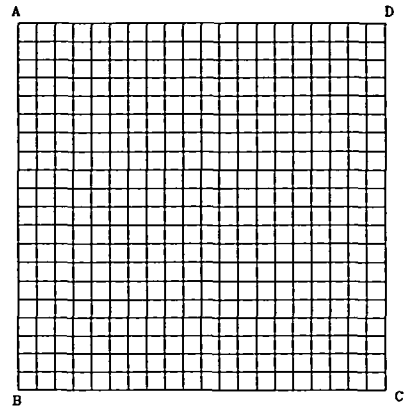

Figure 3 Finite element mesh

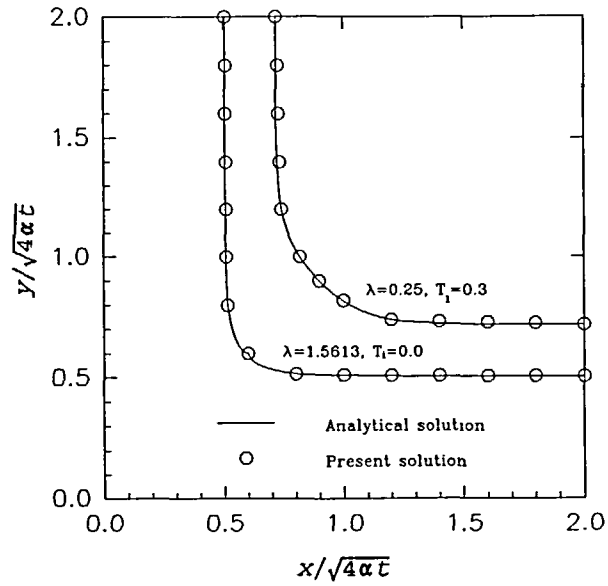

Figure 4 Comparison of the computed interface position with the analytical solution

Computational efficiency tests

The geometry of the phase change material (PCM) is a slice with a radius of 5 cm as shown in *Figure 5*. The PCM is initially at a uniform temperature of 20°C with side AB and AC insulated. On the circumferential side, BC, there is heat convection with the heat transfer coefficient varying linearly, from 17.5 to 87.5 W/m^2·°C, from point B to C. The ambient temperature is −23.6°C. The thermophysical parameters are as follows:

$k_s = 1.55$ W/m·K, $k_l = 0.5$ W/m·K, $c_s = 1240$ J/kg·K, $c_l = 2370$ J/kg·K,
$\rho = 960$ kg/m^3, $\lambda = 167400$ J/kg, $T_m = -1.8$°C.

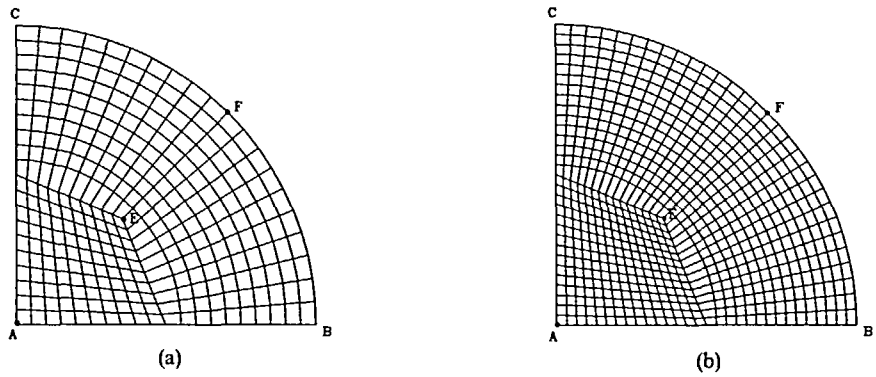

Figure 5 Finite element mesh

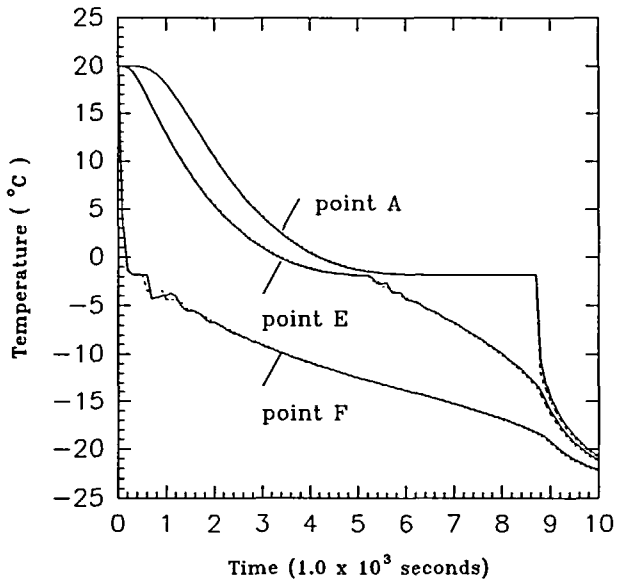

Figure 6 Comparison of temperature histories at some selected points

Computations were carried out using 300 elements and 331 nodes with a time step of 10 seconds (case 1) and 675 elements and 721 nodes with a time step of 5 seconds (case 2). The finite element meshes are illustrated in *Figure 5* (a and b). For comparison, both symmetrized and unsymmetrized global matrices with both stabilized one-point and four-point quadrature are tested for each case. All the computations were carried out with a Packard Bell 486 Personal Computer.

Figure 6 displays the comparison of the temperature histories of points A, E and F between the two cases. The solid lines are for case 1 (300 elements) and the dashed lines for case 2 (675 elements). It can be seen that there is little difference between the results of using 300 elements with a time step of 10 seconds and 675 elements with a time step of 5 seconds.

The execution time, memory requirement, as well as averaged iteration number in each time step for the two cases are listed in *Table 1.*

Table 1 Comparison of computing time and memory requirement

		Iterations per time step	Execution time	Time saved	Memory required in words	Memory saved
Case 1: Elements = 300, Nodes = 331, Δt = 10 s, time step number = 1020						
Unsymmetric matrix	4-point	3.04	2368	52.8%	24999	26.3% Based on 1-point quadrature
	1-point	3.04	1118		24990	
Symmetric matrix	4-point	3.94	2788	58.0%	18424	
	1-point	3.94	1170		18415	
Case 2: Elements = 675, Nodes = 721, Δt = 5 s, time step number = 2040						
Unsymmetric matrix	4-point	3.13	13616	41.9%	60788	34.4% Based on 1-point quadrature
	1-point	3.12	7907		60779	
Symmetric matrix	4-point	4.04	14396	50.5%	39836	
	1-point	4.04	7120		39854	

From this table it can be seen that in case 1 the stabilized one-point quadrature algorithm has the same convergence speed as four-point quadrature and saves 52.8% and 58.0% execution time, respectively, for both unsymmetrized and symmetrized global matrices. For case 2, the stabilized one-point quadrature algorithm saves 41.9% and 50.5% for unsymmetrized and symmetrized global matrix, respectively.

Using the stabilized one-point quadrature algorithm, for case 1 the execution times are nearly the same for unsymmetrized and symmetrized cases, while the memory requirement is 24990 single precision words for unsymmetrized case, but only 18415 single precision words for symmetrized case. The saving of memory requirement is 26.3% using the symmetrized global matrix. For case 2, using symmetrized global matrix, the saving of memory requirement is 34.4%; and there is a 9.95% saving of execution time although the iteration number in each time step is increased due to the treatment of symmetrization. It is clear that the more the nodes of the problem, the more the saving of memory requirement using symmetrized global matrix since only the upper triangle of the global matrix needs storage elements after symmetrization. Numerical experiments proved that although the convergence speed is slowed down due to the treatment of symmetrization, the savings in execution time increase with the increase of total node number using symmetrized global matrix. This is due to the fact that the higher the node number, the bigger the ratio of the computational work required in equation solving to total computational work.

Numerical experiments also proved that the difference of the results between one-point and four-point quadrature algorithm were only observed in decimal places of the temperature values.

It should be noted that the zigzag shapes in the temperature history curves in *Figure 6* are caused by the enthalpy model itself and is a drawback of the enthalpy model used. This drawback can partly be eliminated by refinement of the computational mesh.

CONCLUSIONS

The finite element method was used for the solution of the enthalpy model for phase change heat transfer by conduction. An efficient simultaneous iteration procedure was developed for

the final discrete algebraic equation system. A one-point quadrature integration scheme was incorporated into this procedure, leading to a significant saving in the computing time. Numerical examples have demonstrated the accuracy and efficiency obtainable with this new procedure.

REFERENCES

1 Shamsundar, N. and Sparrow, E. M. Analysis of multidimensional conduction phase change via the enthalpy model, *J. Heat Transfer, Trans. ASME*, **97**, 333–340 (1975)
2 Comini, G., Del Giudice, S., Lewis, R. W. and Zienkiewicz, O. C. Finite element solution of nonlinear heat conduction problems with special reference to phase change, *Int. J. Numer. Meth. Eng.*, **8**, 613–624 (1974)
3 Morgan, K., Lewis, R. W. and Zienkiewicz, O. C. An improved algorithm for heat conduction problems with phase change, *Int. J. Numer. Meth. Eng.*, **12**, 1191–1195 (1978)
4 Comini, G., Del Giudice, S. and Saro, O. A conservative algorithm for multidimensional conduction phase change, *Int. Numer. Meth. Eng.*, **30**, 697–709 (1990).
5 Liu, W. K. and Belytschko, T. Efficient linear and non-linear heat conduction with a quadrilateral element, *Int. J. Numer. Meth. Eng.*, **20**, 931–948 (1984)
6 Liu, W. K., Ong, J. S. and Uras, R. Z. Finite element stabilization matrices—A unification approach, *Comp. Meth. Appl. Mech. Eng.*, **53**, 13–46 (1985)
7 Zienkiewicz, O. C. and Taylor, R. L. *The Finite Element Method*, 4th Ed., Vol. 1, McGraw-Hill, London (1989)
8 Dalhuijsen, A. J. and Segal, A. Comparison of finite element techniques for solidification problems, *Int. J. Numer. Meth. Eng.*, **23**, 1807–1829 (1986)
9 Hogg, M. A comparison of two- and three-level integration schemes for non-linear heat conduction, in *Numerical Methods in Heat Transfer (Eds. R. W. Lewis, K. Mogan and O. C. Zienkiewicz)*, Wiley, Chichester, pp. 75–90 (1981)
10 Bathe, K. J. *Finite Element Procedures in Engineering Analysis*, Prentice-Hall (1982)
11 Hughes, T. J. R., Pister, K. S. and Taylor, R. L. Implicit-explicit finite elements in nonlinear transient analysis, *Comp. Meth. Appl. Eng.*, **17/18**, 159–182 (1979)
12 Pham, Q. T. The use of lumped capacitance in the finite-element solution of heat conduction problems with phase change, *Int. J. Heat Mass Transfer*, **29**, 285–391 (1986)
13 Luikov, A. V. *Analytical Heat Diffusion Theory*, Academic Press, New York (1968)
14 Budhia, H. and Kreith, F. Heat transfer with melting or freezing in a wedge, *Int. J. Heat Mass Transfer*, **16**, 195–211 (1973)